The Brownian Motion

Adrien Cortés, Victor Letzelter, Hugo Besson

July-January 2020-21

Table des matières

1 Introduction, description **2**
1.1 Context 2
1.2 Aim of the project 2

2 Brownian Motion in Physics **2**
2.1 Mathematical definition 2
2.2 Physical approach by experiment : Langevin's theory 2

3 Experience and results **4**
3.1 Context and aims 4
3.2 Protocol 4
3.2.1 Observation of the Brownian trajectories of particles 4
3.2.2 Pointing the particles 5
3.2.3 Particle diameter measurement 6
3.3 Calculation of the Avogadro Number 6
3.3.1 Other possibility for the calculus of D 7
3.3.2 Filtration du Drift 7
3.3.3 Results 10
3.4 Properties to verify, available data 10
3.4.1 Definitions 10
3.5 Available data 10
3.6 Checking the hypothesis 10
3.6.1 Increases that follow a normal distribution 10
3.6.2 Independence of increases 12
3.6.3 Continuity of $t \to X_t(\omega)$ 12
3.7 Simulation from the estimated parameters 15
3.8 Conclusions and questions about the experiment 15

4 Heat equation in finance **18**
4.1 Heat equation 18
4.2 An application of this result and verification 18
4.3 Finance : Black-Scholes model 20
4.3.1 The financial market 20
4.3.2 Les options 20
4.3.3 Black-Scholes Model 21

5 Estimation of market parameters **21**
5.1 Volatility, trend 21
5.2 Implied volatility 23
5.2.1 The theory 23
5.2.2 A simple approach, an iterative dichotomous algorithm 25

6 Conclusion **27**

7 Instructions for use **27**

8 Appendices **27**
8.1 Appendix 1 : Establishing the expression for Avogadro's number 27
8.2 Annex 2 : Itô calculus and heat equation 28
8.3 Annex 3 : R Code, Calcul of historical volatility and the trend on a market 28
8.4 Annex 4 : prediction of a Geometric Brownian by the heat equation 29

1 Introduction, description

1.1 Context

In the summer of 1827, the Scottish naturalist Robert Brown saw very small particles in the fluid inside the pollen grains of Clarkia pulchella, which were moving in an apparently chaotic manner. This physical phenomenon has given rise to mathematical and physical models. The first mathematical description was given by Louis Bachelier in 1900. Pierre Langevin developed a theory in 1906 linking the displacement of these particles to Einstein's diffusion coefficient. It is in a distant field that we today find Brownian motion. In finance, it is used as a basis for modelling the dynamics of stock market prices. The very large number of transactions, i.e. purchases or sales of financial assets, produces small variations in the price of this asset, which can be compared to variations in the position of a particle subject to Brownian motion. Several mathematical models for the description of more complex financial products have as a fundamental assumption that the variation of the price of a financial asset follows a Brownian motion.

In this report, we will present the important aspects of our Technical Project. We will discuss the mathematical, physical and financial theory needed to understand the analogy between these areas.

1.2 Aim of the project

Our project has many goals :

— (1) Understanding the Brownian Motion in its mathematical and physical description and its relevance to financial mathematics.

— (2) Carrying out a physical experiment to visualise Brownian motion and derive results based on Langevin's theory, as well as a numerical simulation of this phenomenon.

— (3) Applying the knowledge of (1) and (2) to study the Black-Scholes model and deduce the characteristics of stock prices.

— A physical experiment allowing to characterise the Brownian motion and to deduce an approximation of the Avogadro number

— A set of functions to calculate the different characteristics of a stock price : volatility, trend and implied volatility from an option price.

We would like to thank Mr. TOUBOUL who accepted to be our tutor without being an expert in the field, and the brilliant Mr. FERRIERES and Mr. BAY, who made us understand the scientific richness of such a subject. We would also like to thank Mrs. Lara LECLERC who allowed us to carry out our experiment at the Centre d'Ingénierie et de Santé des Mines de Saint-Etienne and Mr. BOSCH who advised us on its development.

2 Brownian Motion in Physics

2.1 Mathematical definition

Définition 1 (Brownian Motion)**.** *A**Brownian Motion** is a stochastic process, i.e a sequence of random variables $(B_t)_{t\geq 0}$ assumed to be defined on a probability space $(\Omega, \mathcal{T}, \mathbb{P})$ in values in $(\mathbb{R}, \mathcal{B}(\mathbb{R}))$ with the following properties :*

- $B_0 = 0$
- $\forall (t,s) \in (\mathbb{R}^+)^2, \quad s < t \Rightarrow B_t - B_s \hookrightarrow \mathcal{N}(0, t-s)$
- *B is incrementally independent, i.e. for any $n \in \mathbb{N}$, for all $0 = t_0 < t_1 < ... < t_n$, the random variables $(B_{t_n} - B_{t_{n-1}}), ..., (B_{t_1} - B_{t_0})$ are independants.*
- *For $\omega \in \Omega$, the function $t \rightarrow B_t(\omega)$ is almost surely continuous on $\mathbb{R}^+$*

A Brownian motion is a sequence of random variables that satisfy certain assumptions. This mathematical definition does not allow to easily grasp the physical reality of a Brownian particle ; this is then clarified in the next section.

2.2 Physical approach by experiment : Langevin's theory

The physical approach to Brownian motion using Langevin's theory makes it possible to describe the movement of a particle subjected to a very large number of collisions and to deduce physical quantities.

Let us consider a "large" particle immersed in a fluid (cf FIGURE 1) consisting of much smaller particles. The radius of the Brownian particle is typically : $10^{-9}m < a < 10^{-7}m$. The agitation of the large

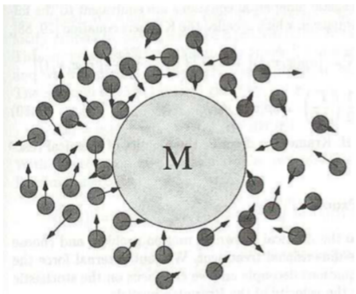

FIGURE 1 – Brownian Particle

particle is much slower than that of the small particles surrounding it, resulting in rapid and random collisions due to local density variations in the fluid (order of magnitude : one collision every $10^{-12}s$; in comparison, our eyes can capture a maximum of 30 images per second).

We deduce from the fundamental principle of dynamics (PFD) applied to this particle, that it obeys the Langevin equation [13] :

$$m\frac{d\mathbf{v}}{dt} = -\gamma\mathbf{v} + \boldsymbol{\eta}(t) \tag{1}$$

where :

— $\mathbf{v}$ is the velocity vector of the centre of mass of the particle.

— γ is the friction coefficient, which according to Stokes' law is $gamma = 6\pi\mu a$ if the Brownian particle is spherical of radius a immersed in a fluid of dynamic viscosity mu, in the case of a laminar and stationary flow notecf [15] page 36 for the demonstration of the expression of the Stokes force.
— m is the mass of the particle
— $\boldsymbol{\eta}(t)$ is a random variable that gives the force resulting from the effect of "background noise" (the effect of the particle's rapid and random collisions with its environment) at time t.

Since the previous equation contains a random term it belongs to the category of *stochastic differential equations* (SDE). Let us give some precision on $\boldsymbol{\eta}(t)$:

With one multiplicative constant, $\boldsymbol{\eta}(t)$ can be assimilated to a Gaussian white noise. That is to say : $boldsymbol\eta(t) = sigma\boldsymbol{\xi}(t)$, where $boldsymbol\xi(t) \sim \mathcal{N}(0, Id)$. Of course, we then have $< boldsymbol\eta(t) >:= \mathbb{E}(\boldsymbol{\eta}(t)) = 0$, the average is here not **not realised with respect to time** but with respect to the different possible realisations of $\boldsymbol{\eta}(t)$.
We therefore have $\mathbb{V}(\boldsymbol{\eta}(t)) = \sigma^2$. We can show that white noise $\boldsymbol{\eta}(t)$ and $\boldsymbol{\eta}(t')$ taken at different times are totally decorrelated :

$$< \boldsymbol{\eta}(t)\boldsymbol{\eta}(t') >= \sigma^2\delta(t-t') \tag{2}$$

where

$$\sigma = \sqrt{2\gamma k_B T} \tag{3}$$

[1] This lack of correlation results from the fact that over a short time interval, say $dt = 10^{-5}$ there are still $10^{-5}10^{12} = 10^7$ collisions. Hence, any "memory effect" will be removed.

From the equation 1, we can show via a judicious change of function detailed in the Appendix 8.1.

$$\boxed{\left\langle \|\vec{r}(t)\|^2 \right\rangle \sim \frac{2dRT}{6\pi\mu a\mathcal{N}_A}t = 2dDt} \tag{4}$$

where

$$D = \frac{RT}{6\pi\mu a\mathcal{N}_A} \tag{5}$$

1. The expression of σ results from the equipartition theorem of the energy applied to the Brownian particle

$$\frac{1}{2}m\left\langle \|\vec{v}(t)\|^2 \right\rangle = \frac{d}{2}k_B T$$

d is the number of dimensions at stake here

The trajectory of a Brownian particle can then be described in terms of a scattering term : the Einstein scattering coefficient D. This coefficient involves the Avogadro number. Thus, if we know the values of R, mu, a, and the temperature T and if we have access to several trajectories, we can make a measurement of the Avogadro number.

In the following section we present the experiment carried out in connection with this theory, allowing us to approach the Avogadro number.

3 Experience and results

3.1 Context and aims

Here we seek to reproduce the historical experiment and characterise the Brownian Motion of these particles. From this experiment, we can deduce certain physical properties.

The aims of this experience are :

1. Allow the observation of the actual Brownian Motion of several particles. (Section 3.2.1)
2. Carrying out the pointing of the trajectory of the particles. (Section 3.2.2)
3. Determining the diameter of the observed particles. (Section 3.2.3)
4. Calculating the Avogadro number thanks to the Einstein diffusion coefficient. (Section 3.3)
5. Checking that the trajectories of the particles are consistent with the properties of Brownian Motion. (Section 3.4)

In the rest of the description, the random variables giving the position of a particle will be supposed to be defined on a probabilized space $(\Omega,\mathcal{T},P)$ with values in $(\mathbb{R},\mathcal{B}(\mathbb{R}))$. Thus, for a $\omega \in \Omega$, $t \to X_t(\omega)$ represents the trajectory followed by one of the particles considered.

3.2 Protocol

3.2.1 Observation of the Brownian trajectories of particles

We decided to observe the Brownian Motion of particles in milk. Milk is an emulsion which contains in suspension, among other substances, microscopic fat globules of fat with dimensions ranging from 0.1 to 10 μm.

To observe the movement of these globules, we observed a drop of milk on a slide under a microscope equipped with a camera connected to a computer.

The material available was :

— Whole milk
— An inverse microscope
— A MOTICAM 1080 pixels webcam compatible with an inverse microscope
— Microscopy equipment (slides, coverslips, etc.)
— A thermometer

The protocol was :

— Dilute the milk 10 to 30 times with distilled water
— Place a drop of diluted milk on the slide, cover with the coverslip and place the preparation on the microscope the microscope slide
— Focus by eye
— Adjust the orientation, intensity and focus of the microscope light source
— Play with the zoom of the camera to try to obtain a large and sufficiently bright image

We have captured several videos where hundreds of particles in perpetual motion can be seen (see Figure 4).

These particles are all the more visible if the contrast of the images is accentuated (cf. Figure 3).

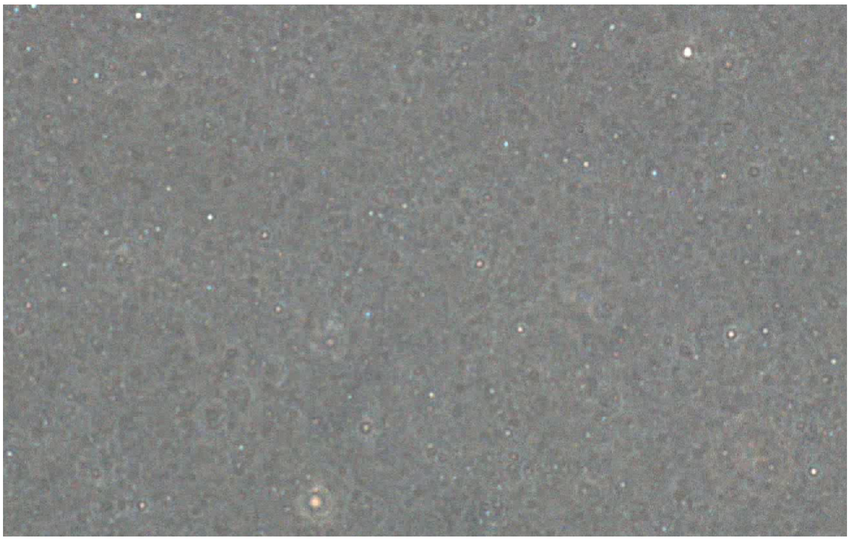

FIGURE 2 – Screenshot of the microscope image

FIGURE 3 – Screenshot of the microscope with contrast

3.2.2 Pointing the particles

To follow the trajectory of the particles, we use the software *Tracker*. As seen previously, the Brownian Motion is defined as a stochastic process, i.e. a sequence of random variables $(X_t, Y_t)_{t \geq 0}$, where, for a given realization (corresponding to a trajectory) $\omega \in \Omega$, $X_t(\omega)$ and $Y_t(\omega)$ provide respectively the abscissa and the ordinate of the particle following this trajectory at time t, taking as origin the initial position of the particle [2]. The calculation of Avogadro's number involves, at a fixed t, the expectation of the random variable $|\overrightarrow{r}(t)\| := \sqrt{X_t^2 + Y_t^2}$. Calculating this expectation, which we will note $< \|\overrightarrow{r}(t)\| >$, amounts to calculating the average, on the whole of the chosen particles, of the positions at the instant t.

As we are considering ensemble averages, we must perform a score on several particles.
[3]

Here we have followed 25 trajectories. We therefore have at our disposal 50 vectors containing an x or y coordinate of a particle. For each pointing, we centre the reference frame on the first position of the particle. We performed the pointing at a frequency of 25 frames per second. The videos used were nearly 50 seconds long, which gave us 1256 positions per particle, or 62800 data in total.

2. When the initial position is chosen as origin, we say that the Brownian Motion is said to be **Standardized**
3. In hindsight, we have realised that the theory of ergodic theory, presented in [9], applies here, which could have allowed us to consider the trajectory of a single particle. This was done in the context of the verification of the Brownian Motion hypotheses in Section 3.6.1.

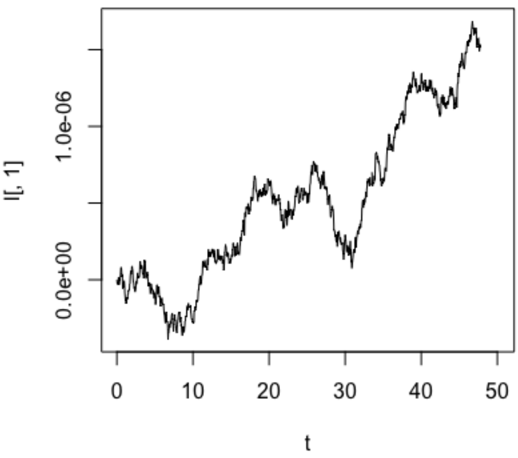

FIGURE 4 – $x_j(t)$ pour une particule j quelconque

3.2.3 Particle diameter measurement

To calculate the Avogadro number we need access to the diameter of the particles. As the diameter of the grease particles is not constant, we pointed to the trajectory of particles of relatively similar size. We then averaged the diameters and used this value to calculate the Avogadro number N_A. The average diameter obtained is of the order of 0.2 μm.

3.3 Calculation of the Avogadro Number

The following relation has been demonstrated on the basis of the Langevin equation [4]. Recall that a represents the (average) radius of the type of particles considered, and μ the dynamic viscosity of the fluid

$$< \|\overrightarrow{r}(t)\|^2 > \sim \frac{2dRT}{6\pi\mu a N_A} t = 2dDt \tag{6}$$

where d is the number of dimensions. Here $d = 2$. And

$$D = \frac{RT}{6\pi\mu N_A}$$

For a particle j, we have two vectors :

$$\begin{bmatrix} x_j(t_0) \\ \dots \\ \dots \\ x_j(t_n), \end{bmatrix}, \begin{bmatrix} y_j(t_0) \\ \dots \\ \dots \\ y_j(t_n) \end{bmatrix}$$

The squared norm of the position for each particle is calculated at each time.

$$\begin{bmatrix} x_j^2(t_0) + y_j^2(t_0) \\ \dots \\ \dots \\ x_j^2(t_n) + y_j^2(t_n) \end{bmatrix} = \begin{bmatrix} r_j^2(t_0) \\ \dots \\ \dots \\ r_j^2(t_n) \end{bmatrix}$$

where $r_j^2(t_n) = \left\|\overrightarrow{r_j(t_n)}\right\|^2$

At each time t_i we calcule the mean of the $r_j^2(t_i)$ on the set of particles, and we get the vector

$$\begin{bmatrix} < r^2(t_0) > \\ \dots \\ \dots \\ < r^2(t_n) > \end{bmatrix}$$

4. This relation is valid provided that the Brownian Motion is Standardised. In the contrary case, it is necessary to replace $\overrightarrow{r}(t)$ by $\overrightarrow{r}(t) - \overrightarrow{r}(0)$ Since our data were not perfectly standardised, we carried out this operation at the beginning of the code

with

$$< r^2(t_i) >= \frac{1}{nombre\ de\ particules} \sum_{j\ particules} r_j^2(t_i)$$

A each time, one can calculate the diffusion coefficient

$$D_i = \frac{1}{2dt_i} < r^2(t_i) >$$

The evolution of D as a function of time is given in Figure 5.

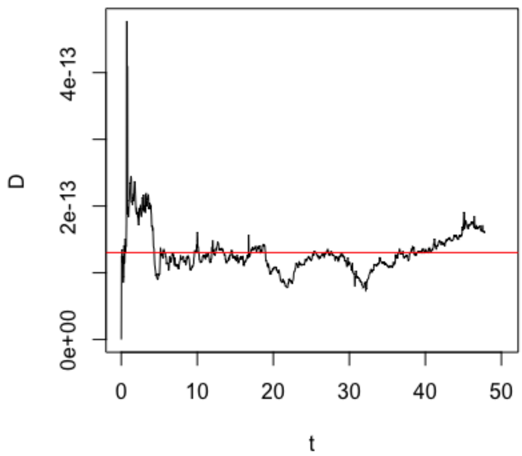

FIGURE 5 – Evolution of the diffusion coefficient over time

Of course, in theory, this coefficient does not depend on time. Nevertheless, the variations of D with respect to its average value (horizontal line in red), remain reasonable. The time average value of D, noted $\bar{D}$ is then used for the calculation of the Avogadro number :

$$N_A = \frac{RT}{6\pi a\mu\bar{D}}$$

3.3.1 Other possibility for the calculus of D

The calculation of the value of D to be included in the formula of N_A can also be done by reasoning from Figure 6 giving the evolution of $< r^2 >$ (average over the 25 particles, as a function of time.

We notice that the evolution of $< r^2 >$ as a function of time is not perfectly linear, but presents two regimes, one for $t < 30\ s$ and the other for $t \geq 30\ s$. One possibility is therefore to reduce the time scale to the interval $[0, 30\ s]$ and then perform a simple linear regression. This is shown in Figure 7. The parameters of the line obtained allow us to deduce that

$$D = 2.86 \times 10^{-14} m^2.s^{-1}$$

We then deduce $N_A = 1.33 \times 10^{22} m^2.s^{-1}$, a less satisfactory estimate than the one presented in paragraph 3.3.3. This can be explained by the fact that linear regression is not necessarily the best tool to use here, since the homoscedasticity hypothesis of the error is not verified.

3.3.2 Filtration du Drift

The reasoning stated previously to obtain Avogadro's number, namely in the first place the equation 6, is based on the hypothesis that the motion of the particle is not subject to *drift*, that is, to a global trend. Let us verify this hypothesis. To do this, let us plot $< x >$, and $< y >$ (averages taken over the sets of particles) against time. This is done in Figure 3.3.2

We can clearly see on Figure 3.3.2 that there is an overall movement : the particles tend to move in the direction of increasing abscissas and decreasing ordinates. To filter this Drift, we act on the matrix, containing the coordinates (abscissa and ordinate) of each particle (marked on the columns of the matrix)

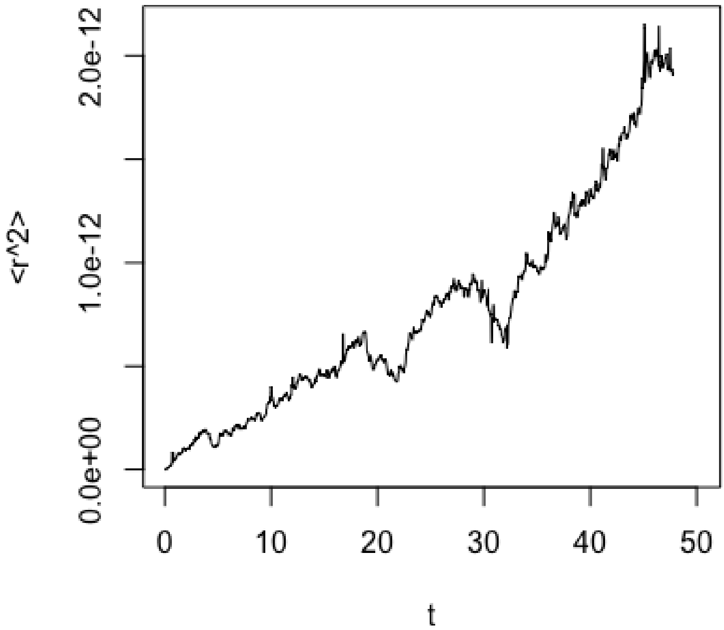

FIGURE 6 – Representation of $< r^2 >$ in funciton of time

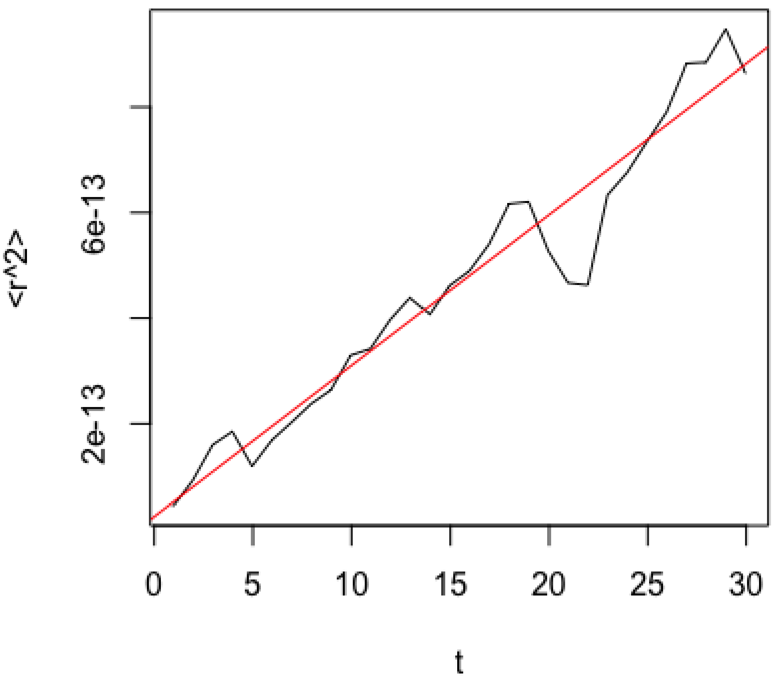

FIGURE 7 – Linear regression performed on the first time range

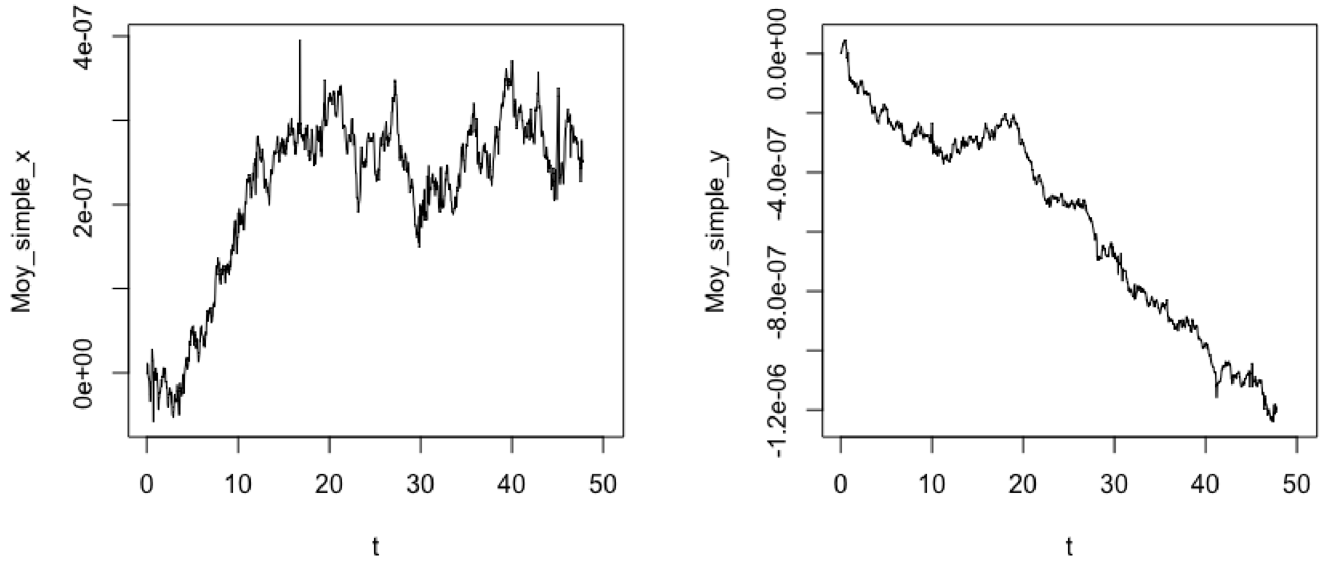

FIGURE 8 – Representation of $< x >$ (left) and of $< y >$ (right) as a function of time

at each instant (marked on the rows of the matrix), which is of size 1256×50. The operations are given in equation [5]

$$\forall (i,j) \in [\![1,1256]\!] \times [1,25], \begin{cases} x_j(t_i) \leftarrow x_j\left(t_i\right) - \left\langle x\left(t_i\right)\right\rangle \\ y_j(t_i) \leftarrow y_j\left(t_i\right) - \left\langle y\left(t_i\right)\right\rangle \end{cases} \quad (7)$$

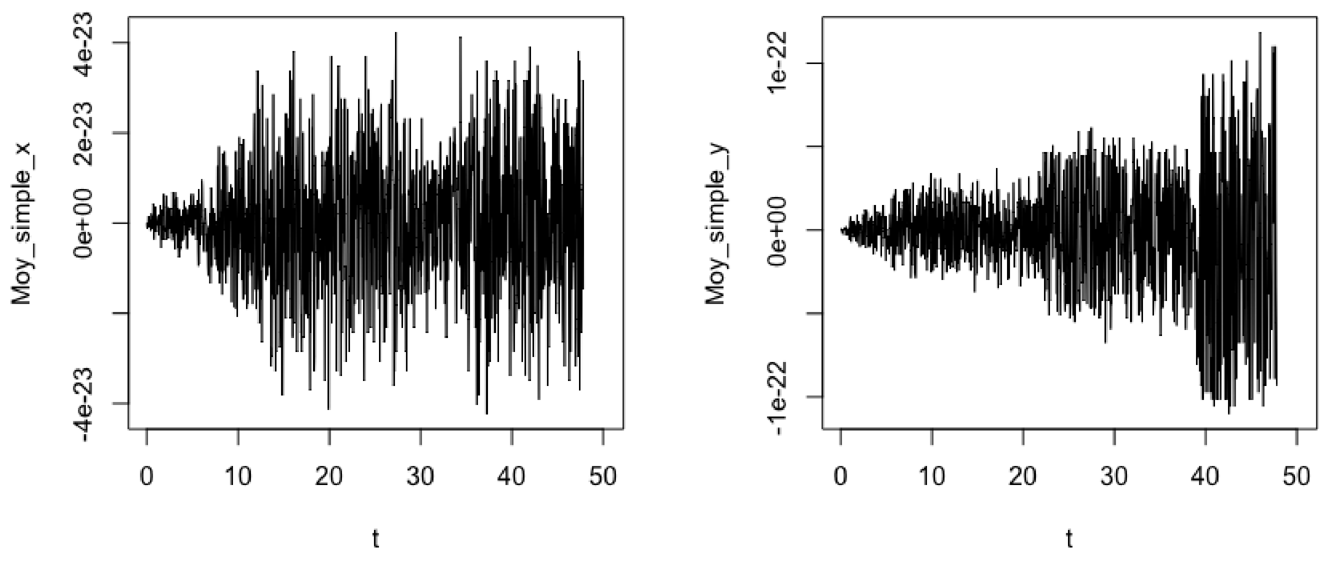

FIGURE 9 – Representation of $< x >$ (left) and of $< y >$ (right) as a function of time after applying the filtration

5. Here, $x_j(t_i)$ represents the abscissa of the j th particle at time t_i. However, it will not be the j th column of the matrix, but the $2j$ th. The matrix contains, in fact, alternately the abscissa and ordinate of each particle.

After applying this filtration, the temporal evolution of $< x >$ and $< y >$ are represented in Figure 9.

The mean values are indeed zero (within 10^{-23}, due to machine rounding errors). The global trend has been removed from the coordinate matrix.

3.3.3 Results

In our case, we had :

- $T = 294.75 \pm 0.1\ K$
- $\mu = \mu_{eau}(T) \sim 10^{-3}\ Pa.s$ [6]
- $a \simeq 0.1\ \mu m$ [7]
- We got (after drift filtration) $< D > \simeq 1.30 \times 10^{-13}\ m^2/s$

We then get :

$$N_A = 2.83 \times 10^{22}\ s^{-1}$$

The value of our approximation is quite far from the theoretical value. We have a relative error of 95. Several factors during the implementation of the experiment and the analysis of the results can explain this discrepancy.

Firstly, we had a problem with the calibration of the microscope. Firstly, we had a problem with the calibration of the microscope, so we had to go back to the laboratory to calibrate and plot these measurements on our data. Moreover we made the hypothesis of a 2D Brownian Motion, but the thickness of the slide is not completely negligible. On the one hand, the expression (6) is no longer correct ($d = 3$) and the value of the root mean square of the particle position does not take into account the motion in the thickness of the blade. Finally, other factors such as edge effects at the level of the blades affecting the movement of the particles or the choice of the estimator.

3.4 Properties to verify, available data

3.4.1 Definitions

The definition of a Brownian motion, given in **Defnition 1** will be useful for this part.

In our case, the position of the particles is governed by two random variables, X_t and Y_t, which follow an Itô process, i.e. they correspond to a relation of the form [8] $dX_t = \mu(X_t, t)dt + \sigma(X_t, t)dB_t$ In the absence of Drift ($\mu = 0$), $X_t = \sigma B_t$.

3.5 Available data

The resulting data set is denoted D. It contains for different positions, i.e. the coordinates x, y, of an observed particle over time. It contains for different positions, i.e. the coordinates x, y, of a particle observed over time.

3.6 Checking the hypothesis

We will check, in our case, the different assumptions related to the Brownian Motion.

3.6.1 Increases that follow a normal distribution

It is assumed that $X_t = \sigma B_t$. Here we study an increase $deltat = 0.04s$. A qq plot and a histogram of the values taken by the random variable are given in Figures 12 and 11, and both show that X_t does follow a centred normal distribution. To determine the parameter σ, we simply took the square root of the variance of the increments (for $t - s = 1$, i.e. increments of 1 unit), considering here only one trajectory (the hypothesis **Ergodic** is used here). We find :

$$\sigma = 1.115545e - 07$$

This can be used to simulate a trajectory similar to ours with a Monte-Carlo method. We show in Figure $ref simulation1d$ the result of the simulation obtained.

6. This is the viscosity of water at 21.6 degrees Celsius from the source [7].
7. We averaged the radii over the different particles. Ideally, we should have taken particles of the same size to gain precision. This could have been possible by using alumina powder instead of milk
8. cf previous PDF for the definition of an Itô process. We consider here the case of a Standardised Brownian Motion

H

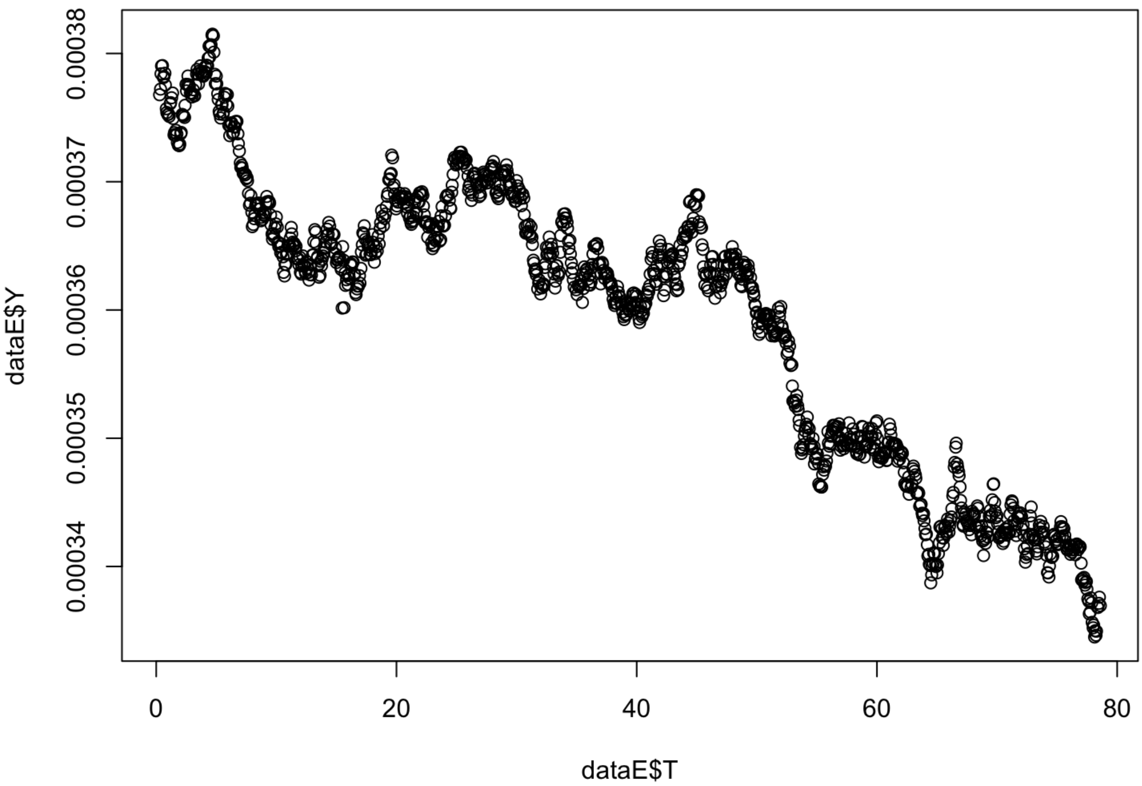

Figure 10 – y-coordinate of the particle as a function of time

H

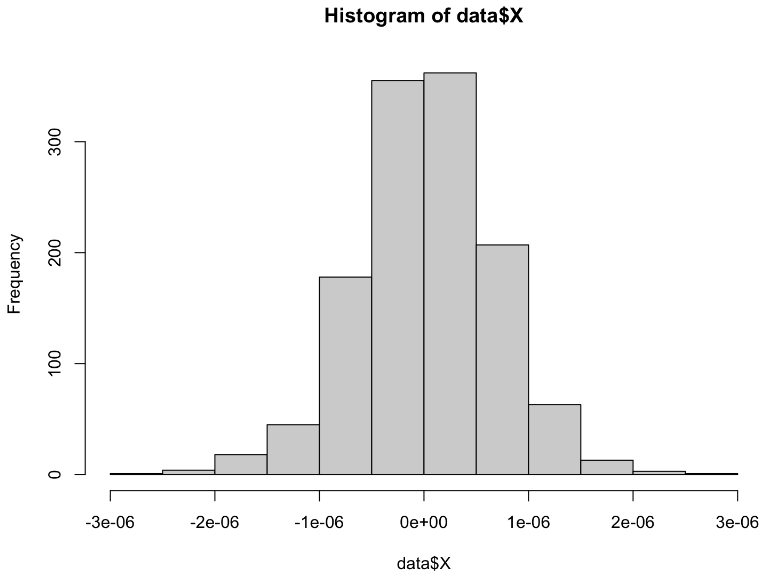

FIGURE 11 – Histogram of $X_t - X_s$, where $t - s = 1$

One can then, for different values of $\Delta t := t - s$ (on the trajectory of a single particle) calculating the corresponding variance of the law. This is done in Figure 13. Note that this variance is proportional to $t - s$.

3.6.2 Independence of increases

The position between two successive observations $X_{t+1} - X_t$ is a random vector which is the result of a large number of shocks. It therefore has stationary statistical properties.
We propose to check the independence of the increases to be able to conclude about the Brownian Motion.

In the case where the series is stationary, i.e. that the increases are of zero covariance, one can be interested in the autocorrelation function.

Recall that the correlation formula r between 2 variables x and y is given by :

$$r = \frac{\mathrm{Cov}(x, y)}{\sigma_x \sigma_y} = \frac{E[(x - E(x))(y - E(y))]}{\sigma_x \sigma_y}$$

In statistics, the autocorrelation of a discrete time series or process x_t is simply the correlation of the process with respect to a time-lagged version of itself. If x_t is a stationary process with expectation μ and standard deviation σ then the definition is :

$$R(k) = \frac{E\left[(x_i - \mu)(x_{i+k} - \mu)\right]}{\sigma^2}$$

In our case, we will study the autocorrelation of the increase series : $A_t = (X_{t+1} - X_t)_{t \geqslant 0}$, and plot the results in Figure 15.

From a naive point of view, the autocorrelation function measures what it calculates, i.e. the internal dependencies of the signal. For example, in the case of images, a highly regular and homogeneous image will have a strong autocorrelation.
In particular, this is interesting for those seeking a model of the signal. Indeed, if this dependence is very weak we can make the hypothesis that the A_t are independent. This is the case here. We thus confirm the hypothesis of independence of the increases.

3.6.3 Continuity of $t \to X_t(\omega)$

Let us consider a realization $\omega \in \Omega$. The continuity of $t \to X_t(\omega)$ can be directly verified graphically. This is what has been done in Figure 10. One can also represent, as an indication, $Y_t(\omega)$ as a function of $X_t(\omega)$ for a given trajectory. This has been done in Figure 14.

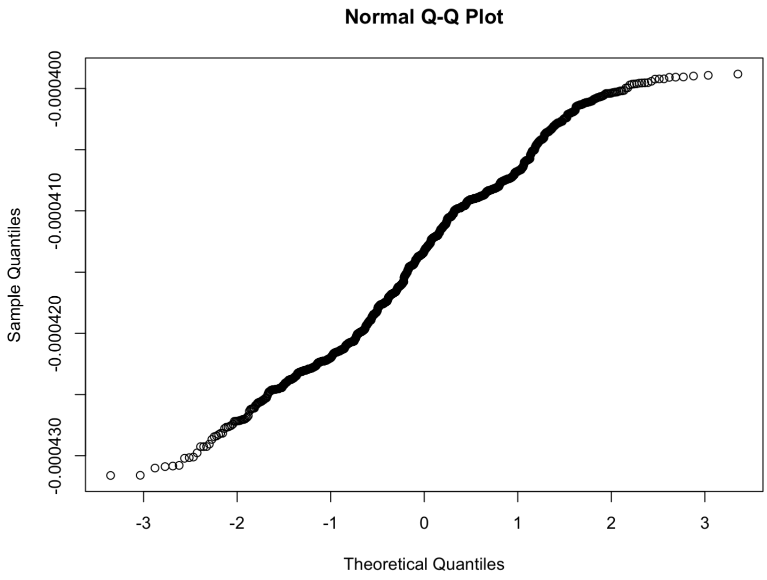

Figure 12 – qq plot for position of the X-axis

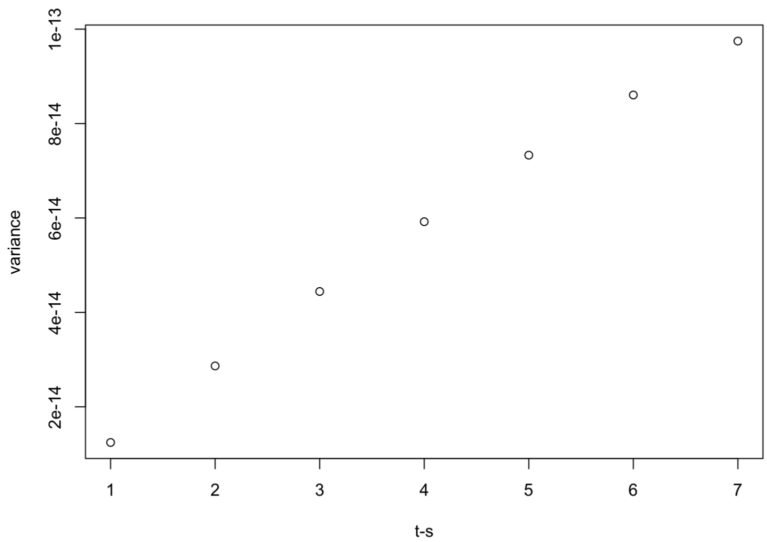

Figure 13 – The variance is well proportional to $t - s$

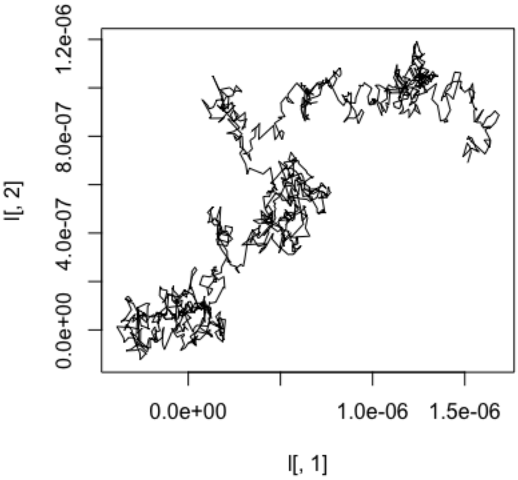

Figure 14 – Spatial evolution of a particle

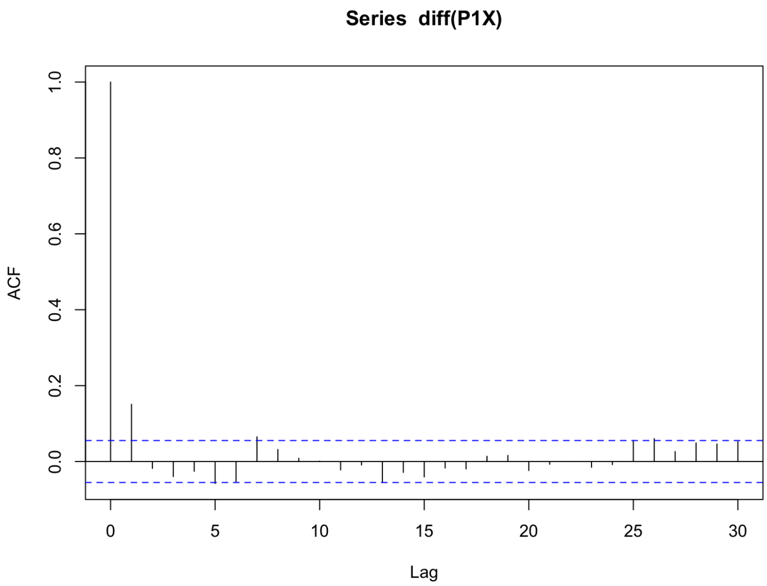

Figure 15 – Autocorrelation of the increase series, this confirms the assumption of independence of the increases

h!

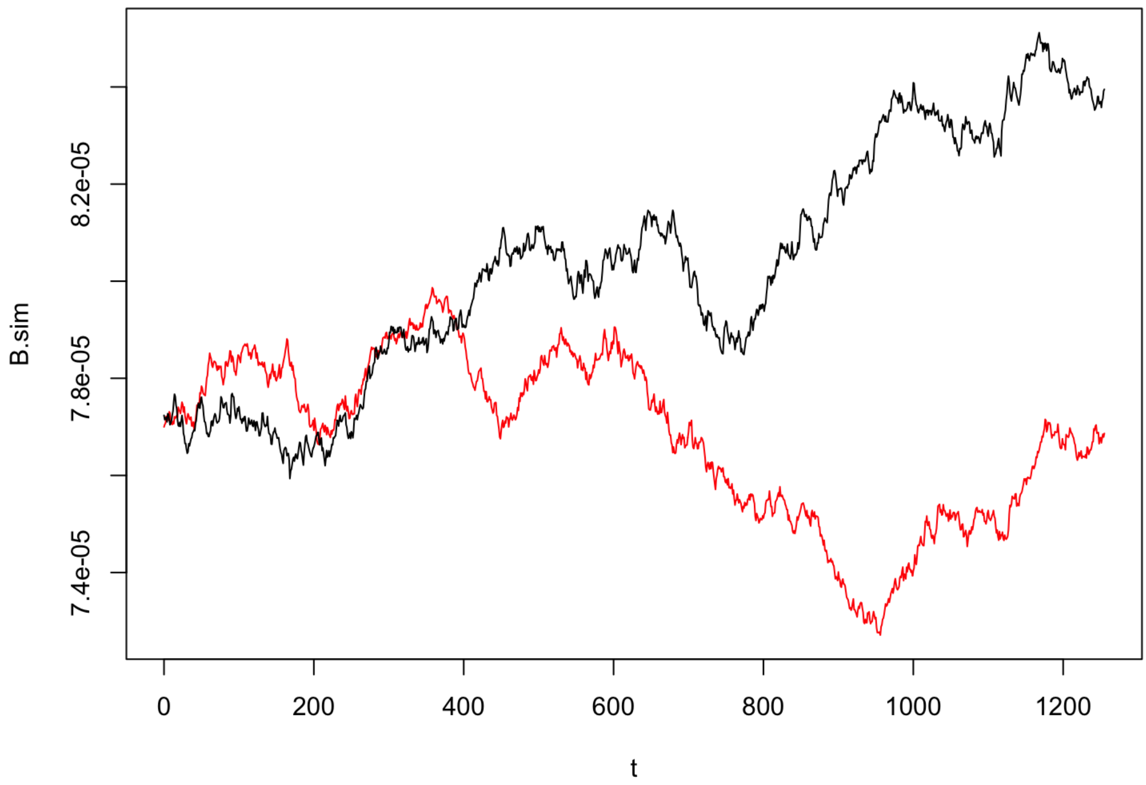

FIGURE 16 – In red, the trajectory with estimated parameters, in black, the real trajectory

3.7 Simulation from the estimated parameters

The strategy for simulating trajectories from the estimated parameters is as follows.

1. We choose a time interval $[0, T]$ and a time step $\Delta t = \frac{T}{n}$.
2. We simulate n realisations of a normal distribution

$$\mathcal{N}(0, \Delta t)$$

.

3. We then get :

$$B_n = B_0 + \sum_{k=0}^{n-1} (B_{(k+1)\frac{T}{n}} - B_{k\frac{T}{n}})$$

4. We then compute $X_t = \sigma_x B_t$ and $Y_t = \sigma_y B_t$.

To simulate a 2D Brownian motion, the reasoning is similar :

$$(X_t, Y_t) = (\sigma_x \sum_{k=0}^{n-1} (B_{(k+1)\frac{T}{n}} - B_{k\frac{T}{n}}), \sigma_y \sum_{k=0}^{n-1} (B_{(k+1)\frac{T}{n}} - B_{k\frac{T}{n}}))$$

3.8 Conclusions and questions about the experiment

This experiment made us notice in particular that the trajectory of a particle, for example that given in FIGURE 10 seems comparable to the trajectory of a financial asset.

Question : How to explain such an analogy ?

h!

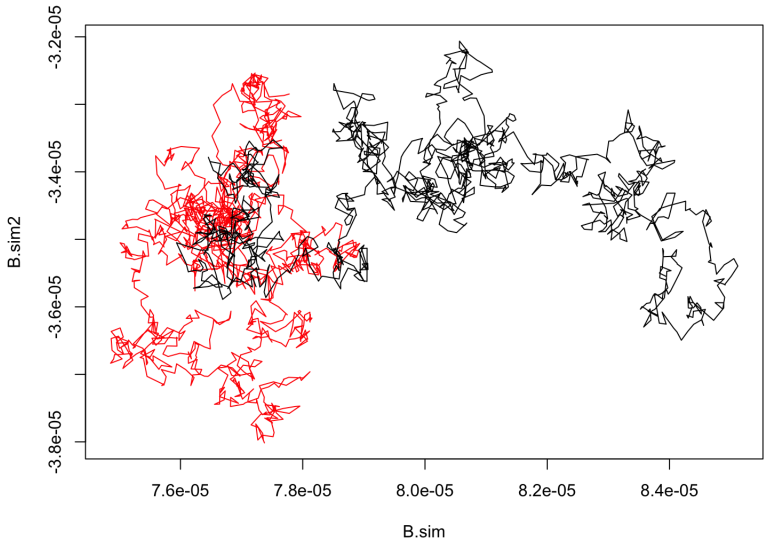

FIGURE 17 – In red, the trajectory with estimated parameters, in black, the real trajectory

Let's focus on the equation (1).

In all generality, it is necessary to place oneself in the case where, in addition to the forces stated above, the particle is immersed in a field of forces $\boldsymbol{F}(\boldsymbol{r})$ footnoteFor example, if we tilt the liquid in which the particle is immersed, we obtain an additional force which results from the difference of potential energy within the liquid. The SDE verified by the position of the particle is :

$$m\ddot{\boldsymbol{r}} = -\gamma\dot{\boldsymbol{r}} + \boldsymbol{F}(\boldsymbol{r}) + \sigma\boldsymbol{\xi}(t)$$

where

$$\sigma = \sqrt{2\gamma k_B T}$$

Under the conditions in which the experiment will be carried out, we will have (cf equation (12))

$$|\gamma\dot{\boldsymbol{r}}| \gg |m\ddot{\boldsymbol{r}}|$$

which means that the force of inertia is negligible compared to the force of friction. In this case, the equation (1) becomes :

$$\gamma\dot{\boldsymbol{r}} = \boldsymbol{F}(\boldsymbol{r}) + \sigma\boldsymbol{\xi}(\boldsymbol{t}) \tag{8}$$

In 1D, the equation (8) is :

$$\frac{dx}{dt} = -\frac{F(x)}{\gamma} + \frac{\sigma}{\gamma}\xi(t)$$

Or else :

$$dx = -\frac{F(x)dt}{\gamma} + \frac{\sigma}{\gamma}dB_t \tag{9}$$

where B_t is a Brownian Motion. Indeed, if we note

$$\mathrm{d}B_t = \xi(t)\mathrm{d}t$$

the reasoning given on pages 78 and 79 of [13] allows us to show rigorously that $(B_t)_{t\geq 0}$ verifies all the properties of a Brownian Motion (properties recalled in **Definition** 1).

The introduction of this sequence of random variables B_t in the preceding equation can be justified mathematically if the continuous sequence of positions taken by the particle can be assimilated to the trajectory of a stochastic process, noted $(X_t)_{t\geq 0}$ [9]. In the following, we will therefore note $\mathrm{d}X_t$ instead of dx.

9. The trajectory, in itself is then noted $t \to X_t(\omega)$

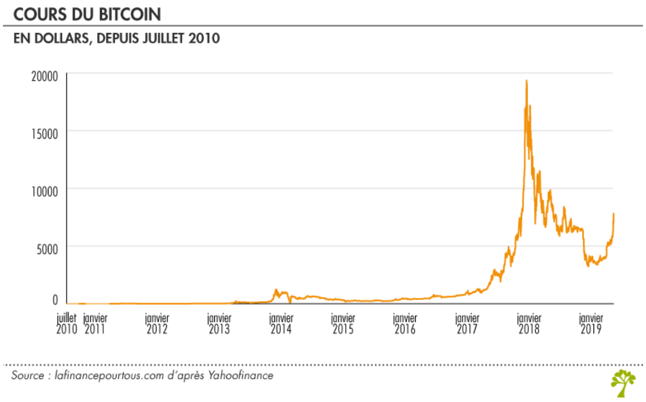

FIGURE 18 – Bitcoin price and its strong upward trend in January 2018

FIGURE 19 – Boeing action price (in dollars) (from [24]) which suffered from sharp decline during the Covid 19 crisis in March 2020

The equation 9 then takes the following very general form [***Itô's Process***]

$$\mathrm{d}X_t = \mu(X_t, t)\mathrm{d}t + \widetilde{\sigma}(X_t, t)\mathrm{d}B_t$$

[10] where we identify the *Drift* (i.e. the global *tendency* of the motion) $\mu(X_t, t) = -\frac{F(x)}{\gamma}$ and the *volatility* (i.e. the amplitude of the Brownian Motion) $\widetilde{\sigma}(X_t, t) = \frac{\sigma}{\gamma} = \sqrt{\frac{2k_BT}{\gamma}} = \sqrt{2D}$

We will see later that the price of a stock market asset $(S_t)_{t\geq 0}$ also follows an Itô process, it is a geometric Brownian Motion.

Définition 2 (Geometric Brownian Motion)**.** *Let $(S_t)_{t\geq 0}$ a stochastic process, and $\mu, \sigma \in \mathbb{R}$. We say that $S := (S_t)$ is a geometric Brownian if it is an Itô process in the form*

$$\frac{\mathrm{d}S_t}{S_t} = \mu \mathrm{d}t + \sigma dB_t$$

We can then show (cf [23] page 40) the following proposition.

Proposition 1. *If (S_t) is a geometric brownian motion with parameters μ and σ, then :*

$$S_t = S_0 \exp\left[(\mu - \frac{\sigma^2}{2})t + \sigma B_t\right]$$

The parameters μ and σ can be interpreted in the same way as for the pollen particle in the liquid.

- μ will represent the global trend of the market : we will have $\mu > 0$ if the trend is *bullish* (see Figure 18 for an example), i.e. if the price has a tendency to rise globally, $\mu < 0$ if the trend is bearish (see Figure 19), and $\mu = 0$ during a period of *range*, when the average price value is zero.
- σ will correspond to the amplitude of the Brownian Motion, i.e. the volatility of the market.

It will be a matter, in paragraph 5.1, of finding a method for estimating these parameters.

We have therefore established a first link between Brownian Motion used in Physics and that used in Finance. Let's continue to establish an analogy between these two domains using one of the best known equations in Physics : *the heat equation.*

10. A process that verifies such a differential equation is, by definition, an Itô process.

4 Heat equation in finance

4.1 Heat equation

In this section, we will show the link between the heat equation used in Physics and that used in Finance to describe diffusion processes.

Définition 3 (Heat equation)**.** *A heat equation in d dimensions is any PDE of the form*

$$\frac{\partial u}{\partial t} = K\Delta u$$

where $u : \mathbb{R}^d \times \left]0, \infty\right[\rightarrow \mathbb{R}$ is a function of class C_b^1 [11] in time and C_b^2 in space, and $\Delta u = \sum_{i=1}^{d} \frac{\partial^2 u}{\partial x_i^2}$.

In the following, we will consider the dimensionless heat equation in which $K = 1/2$.

We will make the reader feel the power of these tools in a first approximation of the Itô Lemma excessively used in financial mathematics and involving the Brownian Motion.

Let $g(t, x)$ the Gaussian density of variance t. We note

$$q(t, x, y) = \frac{1}{\sqrt{2\pi t}} \exp -\frac{(y-x)^2}{2t} = g(t, x-y)$$

the transition density of Brownian Motion
[12]

It is, visually, the probability that the Brownian Motion is in y knowing that t moments before, it was in x, it is also the conditional density

$$P\left(B_{t+s} \in y \pm dy \mid B_s = x\right) = q(t, x, y)dy$$

The transition density q satisfies the forward equation

$$\frac{\partial q}{\partial t}(t, x, y) = \frac{1}{2}\frac{\partial^2 q}{\partial y^2}(t, x, y)$$

and the backward equation

$$\frac{\partial q}{\partial t}(t, x, y) = \frac{1}{2}\frac{\partial^2 q}{\partial x^2}(t, x, y)$$

These two equation are fundamental in finance [13]

Given an initial condition $u(\cdot, 0) = h$, the function u can be obtained by the convolution product [11]

$$u(x, t) = g(t, x) * h = \int_{\mathbb{R}} g(t, x-y)h(y)\mathrm{d}y$$

In the following, we will translate the origin of the times in order to adapt to the notation used in finance. The initial condition will be taken at time t and T will designate an instant $T \geq t$

It can be shown (see Annex 8.2) that the approach is analogous in finance. The function to be predicted will then not be u, but $\mathbb{E}\left(f\left(B_T\right) \mid B_t = x\right)$, where f is any borelian function.

This leads to the following basic result : **If f is a C_b^1 function in time C_b^2 in space,** $\mathbb{E}\left(f\left(t, x+B_t\right)\right) = f(0, x) + \int_0^t \mathbb{E}\left[\frac{1}{2} f''_{xx}\left(s, x+B_s\right) + f'_t\left(s, x+B_s\right)\right] ds$

4.2 An application of this result and verification

We recall the following fundamental result which will allow us to better understand Itô's lemma :
If f is a C_b^1 function in time C_b^2 in space

$$\mathbb{E}\left(f\left(t, x+B_t\right)\right) = f(0, x) + \int_0^t \mathbb{E}\left[\frac{1}{2} f''_{xx}\left(s, x+B_s\right) + f'_t\left(s, x+B_s\right)\right] ds$$

We propose to carry out a simulation and to see the interest of such a proposal for the prediction.

11. This notation means that the function is of class C^1 and bounded with respect to the variable considered
12. The function g is a solution of the heat equation for $K = 1/2$ and $d = 1$ is the *core of heat* (cf [10].)
13. cf [10]

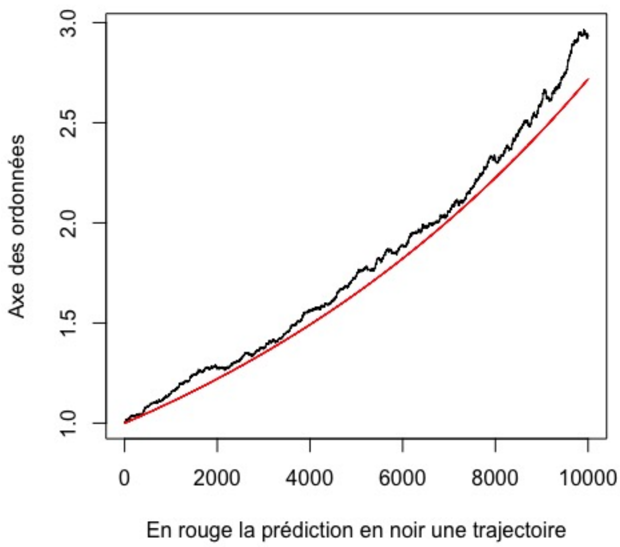

FIGURE 20 – Prédiction de la trajectoire pour $\sigma = 10^{-3}$ et $\mu = 10^{-4}$

The classic choice is : [14]

$$\begin{array}{l} f : (t,x) \longrightarrow \exp((\mu - \frac{\sigma^2}{2})t + \sigma x) \\ \frac{\partial^2 f}{\partial x^2}(x,t) = \sigma^2 \exp((\mu - \frac{\sigma^2}{2})t + \sigma x) \\ \frac{\partial f}{\partial t}(x,t) = (\mu - \frac{\sigma^2}{2}) \exp((\mu - \frac{\sigma^2}{2})t + \sigma x) \end{array}$$

In particular, for $x = 0$

$$\mathbb{E}(f(t,B_t)) = f(0,0) + \int_0^t \mathbb{E}[\mu \exp((\mu - \frac{\sigma^2}{2})s + \sigma B_s)]ds.$$

Then, with the initial condition $f(0,0) = 1$

$$\mathbb{E}[\mu \exp((\mu - \frac{\sigma^2}{2})s + \sigma B_s)] = \mu \exp((\mu - \frac{\sigma^2}{2})s)\mathbb{E}\left(\exp\left(\sigma B_s\right)\right)$$

But :

$$\begin{aligned} \mathbb{E}\left(e^{\sigma B_s}\right) &= \frac{1}{\sqrt{x\pi s}} \int_{\mathbb{R}} e^{-\frac{t^2}{2s}} e^{\sigma t} dt \\ &= \frac{1}{\sqrt{2\pi s}} \int_{\mathbb{R}} e^{\frac{s\sigma^2}{2}} e^{-\left(\frac{t}{\sqrt{2s}} - \sqrt{\frac{s}{2}}\sigma\right)^2} dt \\ &= e^{s\frac{\sigma^2}{2}} \end{aligned} \tag{10}$$

We then get :

$$\mathbb{E}\left(f\left(t,B_t\right)\right) = 1 + \mu \int_0^t \exp\left(\mu s\right) ds$$

And then : [15]

$$\mathbb{E}\left(f\left(t,B_t\right)\right) = e^{\mu t}$$

We obtained for the simulations the result in Figure 20. The power of this method lies in the fact that the prediction is possible even before the trajectory has been traced ! [16]. The instructions for the R code used to carry out this simulation are given in paragraph. 7.

It follows that one can predict with confidence intervals the evolution of any function derived from Brownian Motion.

14. This choice for f is not insignificant : we saw in the proposition 1 that $f(t,B_t)$ is the theoretical expression giving the price of an asset at time t, knowing the two parameters μ and σ which correspond respectively to the trend (global movement of the market) and the volatility (amplitude of the Brownian Motion, of the *bruit* in the market)

15. provided that, of course $\mu \neq 0$

16. It is necessary however that the parameters μ and σ are known

4.3 Finance : Black-Scholes model

Brownian motion plays an important role in the formulation of some financial mathematics models. Before looking at the Black-Scholes model, it is important to recall the main financial concepts that will be used later.

4.3.1 The financial market

We place ourselves in an *organized market*, the contracts are standardized :

— The number of different delivery dates is limited

— The underlyings An underlying is an asset, the price of which will influence the price of a derivative product, for example an Option which is defined in paragraph 5.2.2 are described in detail

— The quotation of the contracts is published continuously

The number of quoted contracts is small and therefore the volumes are larger. The aim is to eliminate counterparty risk. There is a single counterparty : the market's clearing house (low chance of bankruptcy)

A financial asset is a security or contract, usually transferable and tradable, that is capable of producing income or capital gain for the holder in return for taking a certain amount of risk. There are two types of assets :

— **risky assets** : these are assets whose price fluctuates over time.

— **risk-free assets** : their principle is based on the investment of a sum of money in a savings account, which ensures the provision of interest $r < 1$ over a period of one unit of time r (for example, if r is over a period of one year, then it corresponds to the annual interest). Thus if the account has C_0 at time $t = 0$, then at time $t = T$: $C_T = C_0(1+r)^{\frac{T}{\Delta t}}$

The behaviour of the price of a risky asset can be likened to a geometric Brownian Motion. i.e. the variation of the price over time depending on a trend or Drift and a stochastic term modelling the random nature of the small scale variations resulting from the multitude of transactions influencing the price.

The price S_t of an asset then verifies the following stochastic differential equation (Black-Scholes, 1975) : [17]

$$\boxed{\frac{dS_t}{S_t} = \mu dt + \sigma dB_t}\,^{18} \tag{11}$$

With $B = (B_t)_{t\geq 0}$ a standard Brownian Motion, μ the dirft and σ is the volatility.

4.3.2 Les options

The Black-Scholes model is used for the valuation and hedging of options. Options are financial products known as derivatives which give the right to buy or sell a quantity of assets known as the underlying assets, such as shares or currencies for example, during a period and at a price agreed in advance. There are two types of options : call and put options. In our study we focus on call options.

Définition 4 (European Call Option)**.** *A European call option or vanilla option : gives the holder the right (but not the obligation) to buy the underlying asset at :*

— *A due date T*

— *A strike price K*

The price of this option is called the premium, which we will note p. It is paid by the buyer at the time of signing the contract. Moreover, when the buyer holds the share, he immediately sells it at the market price S_T . It is therefore understood that the buyer has a profit only if $K < S_T-$. The buyer buys a call option in anticipation of an increase in the market price of the underlying asset. If the price rises well above $(K+p)$ at expiry : the sale of the shares at S_T at expiry will result in a profit of $S_T - (K+p)$ per share. If the price does not rise above K, then one does not exercise the right to buy the shares and loses p per share.

17. This is a special case of the Itô process, which writes, for a stochastic process $(X_t)_{t\geq 0}$

$$\mathrm{d}X_t = \mu(X_t, t)\mathrm{d}t + \sigma(X_t, t)\mathrm{d}B_t$$

18. Thus we deduce than, at time t fixed, $\frac{dS_t}{S_t} \simeq \frac{S_{t+dt}-S_t}{S_t} \sim \mathcal{N}(\mu dt, \sigma^2 dt)$, if we consider that μ and σ do not depend of S_t

4.3.3 Black-Scholes Model

This model estimates the option premium given the cost of the underlying asset, the strike price, the maturity and the price characteristics of the underlying asset, in particular the volatility. Several assumptions are required to use this model.

It exists at least two assets :

- Risky assets (actions) : the price of this asset follows a Geometric Brownian motion **Brownian Motion**.
- A non-risky asset : the interest rate r is constant, and the asset pays no dividend.

The market follows the following hypothesis :

- No arbitrage (no profit without risk)
- Ability to lend or borrow any amount at the same rate as the non-risky asset
- It is possible to buy or sell any amount of the risky asset
- No transaction cost

Théorème 1. *Under the above assumptions, the price of an option is a solution of the Black-Scholes partial differential equation :*

$$\frac{\partial C}{\partial t} + \frac{1}{2}\sigma^2 S^2 \frac{\partial^2 C}{\partial S^2} + rS\frac{\partial C}{\partial S} - rC = 0$$

Where :

- *$C = C(S,t)$ is the price of the option (Call here)*
- *S is the current price of the underlying asset*
- *σ is the volatility of the asset price*
- *r is the interest rate of the non-risky asset*

The establishment of this partial differential equation is given in Wiki. The Brownian Motion intervenes in the modelling of the underlying asset price, we use the volatility of the price intervening in the differential equation characteristic of the geometric Brownian Motion.

We can then show the following proposition.

Proposition 2. *The general solution of the Black-Scholes equation for a call option is*

$$C\left(S_0, t\right) = S_0 N\left(d_1\right) - K e^{-r(T-t)} N\left(d_2\right)$$

where

- *N is the distribution function of the standard normal distribution*
- $d_1 = \frac{\ln\left(\frac{S}{K}\right) + \left(r + \frac{\sigma^2}{2}\right)(T-t)}{\sigma\sqrt{T-t}}$
- $d_2 = \frac{\ln\left(\frac{S}{K}\right) + \left(r - \frac{\sigma^2}{2}\right)(T-t)}{\sigma\sqrt{T-t}}$

This proposal will be used again when calculating implied volatility, in particular in section 6.2.

5 Estimation of market parameters

5.1 Volatility, trend

As stated in proposition 1, solving the equation 11 under the hypothesis that the volatility σ and the trend μ of an asset are considered constant gives the following expression for S_t the value of the corresponding asset price at time t :

$$S_t = S_0 \exp\left(\mu - \frac{\sigma^2}{2}\right)t + \sigma B_t)$$

We deduce that on a given time interval $[0,T]$ which is discretised by a sequence of instants $0 = t_0 < t_1 < ... < t_n = T$ given (for $n \in \mathbb{N}$ big enough), we have for $j \in [\![2, n]\!]$

$$\ln(S_{t_j}) - \ln(S_{t_{j-1}}) = (\mu - \frac{\sigma^2}{2})\Delta t + \sigma \Delta B \sim \mathcal{N}((\mu - \frac{\sigma^2}{2})\Delta t, \sigma^2 \Delta t)$$

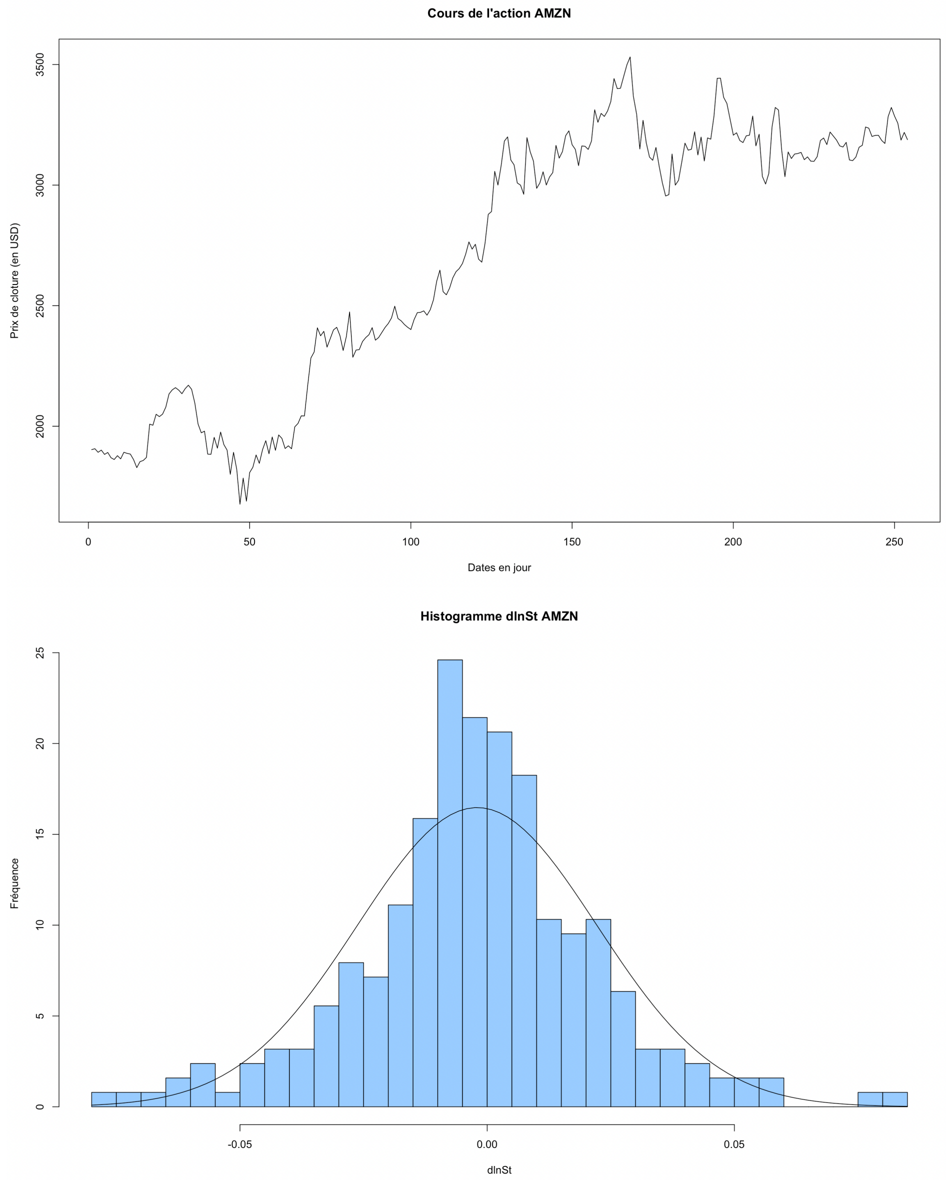

Figure 21 – Top : AMZN share price in USD[20], bottom : Distribution of the $(\ln(\frac{S_t}{S_{t-1}})$ (en échelle journalière) pour l'action AMAZONE sur une fenêtre de 253 jours

The histogram of the $(\ln(S_{t_j}) - \ln(S_{t_{j-1}}))_{j \in [\![2,n]\!]}$ for a given asset thus allows access to the μ and σ parameters of a financial asset.

This numerical study was carried out using the R code given in Appendix 8.3. For the AMAZONE share (AMZN), whose price was extracted from the site [25], the histogram obtained and the price of the corresponding asset are presented in Figure 5.1

This approach can be reproduced on many other assets. In Figure 5.1, the corresponding histograms for the EUR / USD (exchange rate) and for SAFRAN are represented[21].

The calculation of the parameters μ and σ is thus carried out by calculating the average $\tilde{\mu}$ and the standard deviation $\tilde{\sigma}$ and by writing :

$$\begin{cases} \tilde{\mu} = (\mu - \frac{\sigma^2}{2})\Delta t \\ \tilde{\sigma}^2 = \sigma^2 \Delta t \end{cases}$$

Let :[22]

$$\begin{cases} \mu = \frac{2\tilde{\mu} + \tilde{\sigma}^2}{2\Delta t} \\ \sigma = \frac{\tilde{\sigma}}{\sqrt{\Delta t}} \end{cases}$$

21. These stock market data were imported via the site [26]
22. Volatility is a positive parameter

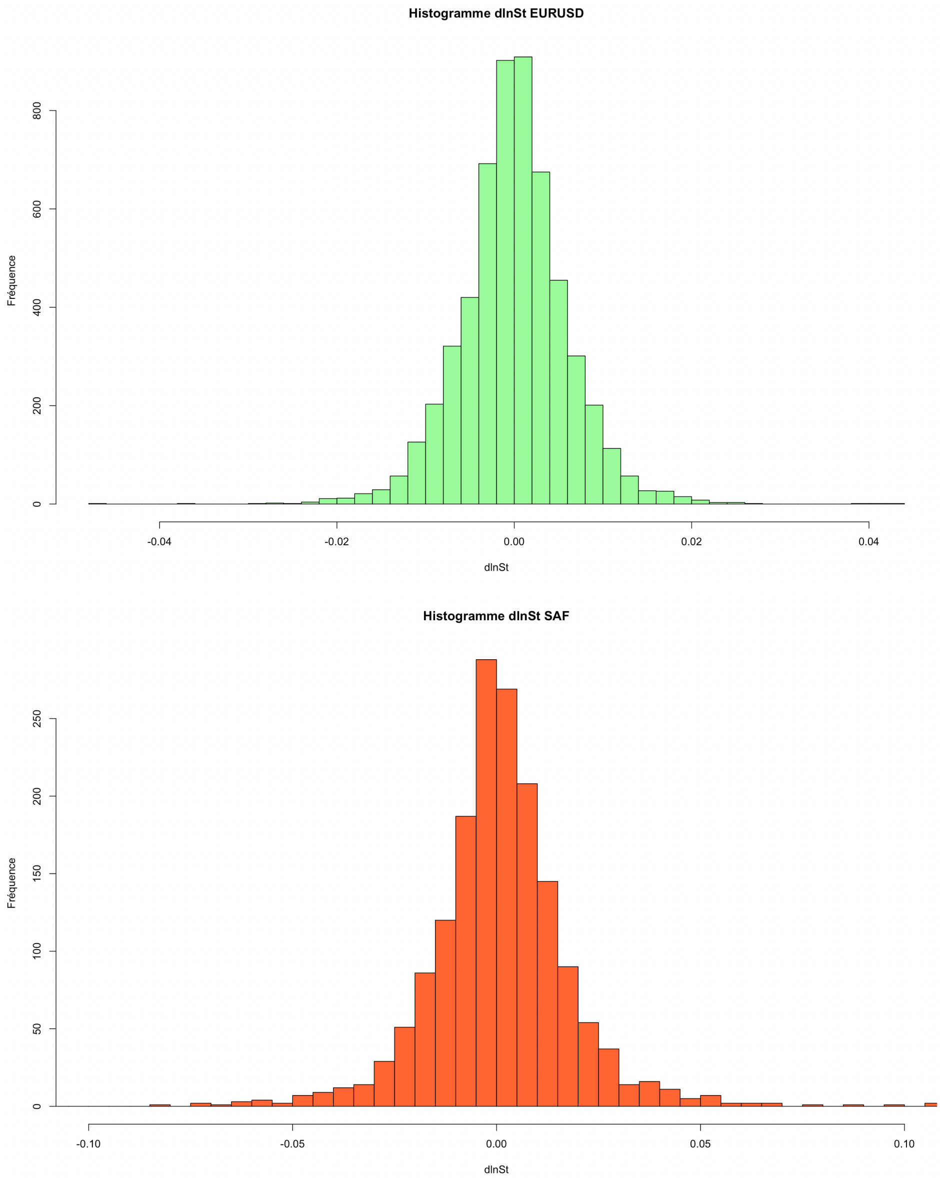

FIGURE 22 – Corresponding histograms for EURUSD (in top) and for SAFRAN (in bottom)

For this calculation, an important parameter is the chosen window (here, this corresponds to the number of days preceding the date of the day involved in the calculation of the standard deviation $\tilde{\sigma}$) for the calculation of the volatility. Indeed, even if the parameters μ and σ have been treated here as constants in the reasoning, one must keep in mind that in reality they are functions of time. If the chosen window is too large, the calculated parameters will not be in line with the current state of the market. Conversely, if the window chosen is too short, we will not find a normal distribution in the histogram (see Figure 23).

Let's focus on the Amazon stock (AMZN). The R code given in the Annex 8.3 allows us to calculate the historical volatility of the asset, over a 20-day window for example. The evolution of the historical volatility obtained over the 60 days preceding Wednesday 6 January 2021 and given in Figure 24.

These historical values are entirely consistent with those found on specialised sites (cf [27]), as shown in Figure 25.

5.2 Implied volatility

5.2.1 The theory

In the Black-Scholes model, the only unobservable parameter is volatility. It should be borne in mind that, in general, we cannot assume constant volatility. We note $\sigma_{\text{impl}}(K,T)$ the implicit volatility. We have just seen that the Black-Scholes price and that of a derivative product verify :

$$C_{BS}\left(S,t,K,T;\sigma_{\text{impl}}(K,T)\right) = C_{\text{Marché}}\left(t,K,T\right)$$

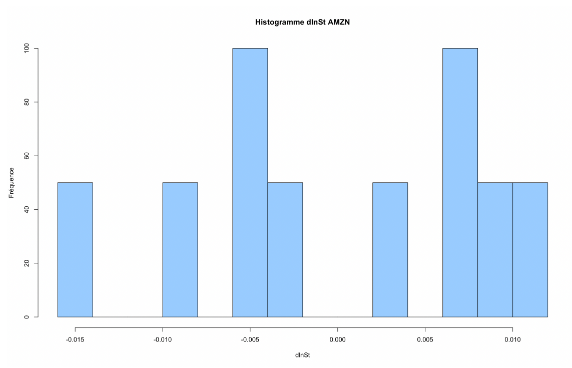

FIGURE 23 – Histogram obtained for the AMZN price for a 10-day window

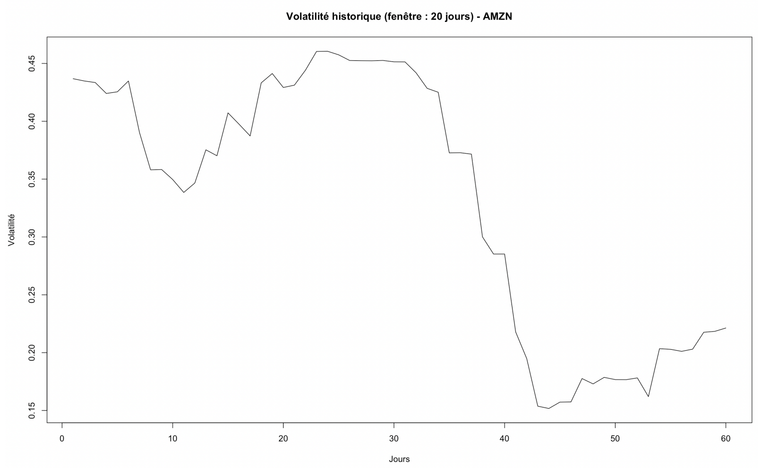

FIGURE 24 – Evolution of the historical Volatility of AMZN over a period of 20 days evaluated with the previous model

FIGURE 25 – Temporal evolution of the volatility of AMZN over a period of 20 days given by the site [27]

It is important to note that $\sigma \rightarrow C_{BS}$: is increasing; option prices increase if volatility increases. Similarly, $\sigma_{athrmimpl}(K,T)$ depends on K and $T-t$, it is not constant. This is the volatility smile. We take, classically :

$$\frac{dS_t}{S_t} = \mu(S,t)dt + \sigma(S,t)dB_t$$

We still have a Black-Scholes PDE for calls :

$$\frac{\partial C}{\partial t} + \frac{1}{2}\sigma(S,t)^2 S^2 \frac{\partial^2 C}{\partial S^2} + rS\frac{\partial C}{\partial S} = rC, \quad t < T$$

with final condition $C(S,T) = \max(S-K,0)$ and solution $C(S,t;K,T)$

5.2.2 A simple approach, an iterative dichotomous algorithm

Calculating implied volatility explicitly is computationally tedious. We have chosen to approximate it as precisely as possible using the algorithm described below. In the following, we will note C being the value of the the Call option on the market).

This method consists of calculating the implied volatility, from the market value of the option, based on the Black Scholes formula. From a bounded range of volatility, we create two adjacent volatility sequences that converge to the real value of volatility. We calculate C_1 for a maximum volatility σ_{Max} and a minimum volatility σ_{min}. These two limits of volatility are initialised by a value close to 0.5, for example, for σ_{Max} and close to 0 for σ_{min}. The value of the option $C_t(\sigma)$ is designated, respectively, by $\text{C}_{\text{Max}} > \text{C}$ for the maximum value of the volatility σ_{max} and by $\text{C}_{\text{min}} < \text{C}$ for the minimum value of the volatility σ_{min}.[23]

Then, we calculate $\text{C}_1(\sigma)$, for each value of the average of the bounds of the volatility interval :

— $\sigma = \frac{\sigma_{Max} + \sigma_{\text{min}}}{2}$

— If $\text{C}_t(\sigma) < \text{C}$ alors $\text{C}_{\text{min}} = \text{C}_t(\sigma)$ et $\sigma_{\text{min}} = \sigma$

— If $\text{C}_t(\sigma) > \text{C}$ alors $\text{C}_{\text{Max}} = \text{C}_t(\sigma)$ et $\sigma_{\text{Max}} = \sigma$

This iterative calculation stops when the gap $\varepsilon_t = |\text{C}_t(\sigma) - \text{C}|$ becomes *leq* than a given value ε given (10^{-7} for instance).

The purpose of our algorithm will be twofold :

— Calculating the price of a call option using the formula given in proposition 5.2.2.

— Knowing the price of a call option on the market, deduce the value of the volatility (it is then the implied volatility.

Hence our algorithm :

```
import numpy as np
import scipy.stats as si
import sympy as sy
from sympy.stats import Normal, cdf
from sympy import init_printing
init_printing()

##Calculation of a Call option price by the Black-Scholes model

def euro_vanilla_call(S, K, T, r, sigma):

    #S: Price of the action
    #K: Strike price
    #T: Time remaining before the option expires, as a percentage of a year
    #r: interest rate
    #sigma: implied volatility

    d1 = (np.log(S / K) + (r + 0.5 * sigma ** 2) * T) / (sigma * np.sqrt(T))
    d2 = (np.log(S / K) + (r - 0.5 * sigma ** 2) * T) / (sigma * np.sqrt(T))
```

23. It is calculated by the Black Scholes formula, or by any other parametric model.

```
    call = (S * si.norm.cdf(d1, 0.0, 1.0) - K * np.exp(-r * T) * si.norm.cdf(d2, 0.0, 1.0))

    return call


##the precision function calculates the implied volatility with an eps precision

def precision(eps,C,S,T,K,r):
    #same parameters except that here eps is the precision and C is the real price of the option
    sigma_min = 0
    sigma_max=1
    sigma = 0.5
    C_BS = euro_vanilla_call(S, K, T, r, sigma)
    n=0
    while abs(C_BS-C)>eps and n<1000:
        sigma = (sigma_min +sigma_max)/2
        C_BS = euro_vanilla_call(S, K, T, r, sigma)
        if C_BS<C:
            sigma_min = sigma
        if C_BS>C:
            sigma_max=sigma
        n+=1
    return (sigma)
```

An example of a platform where it is possible to buy options is given in Figure 5.2.2. The objective here is not of course to describe all the elements of the interface, but simply a few key variables : In the first column, several K option strike prices are proposed. The columns *Bid* and *Ask* correspond, in French, to the offer and the demand. transaction between a buyer and a seller of options can only take place if the corresponding price is between these two values. On the buyer's side, *Ask* corresponds to the option's purchase price and *Bid* to the sale price. The implicit volatility σ is given here and is worth 34.6 percent. Finally, the options expire in 2 days ($T = frac2252$ Once again, we express T in stock market years (252 days)). Finally, the price of AMZN at the corresponding time is $S_t = 3138.38$, and the interest rate r is constant during this period and is 1 percent. Consider then the first line of the image, where $K = 3090$, $C = 63.6$.

Amazon.com Inc (AMZN)
3,138.38 -80.13 (-2.49%) 01/06/21 [NASDAQ]
3,146.50 x 1 3,148.00 x 8 POST-MARKET **3,148.00 +9.62 (+0.31%)** 18:44 ET
OPTIONS PRICES for Wed, Jan 6th, 2021 Alerts Watch Help
Make this my default view

Expiration: 2021-01-08 (w) Near-the-Money Stacked **download**

2 Days to expiration on **2021-01-08** Implied Volatility: **34.60%**

Calls

Strike	Moneyness	Bid	Midpoint	Ask	Last	Change	%Chg	Volume	Open Int	Vol/OI	IV	Last Trade	Links
3,090.00	+1.54%	61.85	62.73	63.60	62.92	-72.35	-53.49%	65	117	0.56	35.93%	01/06/21	⋮
3,095.00	+1.38%	58.10	59.00	59.90	58.40	-62.90	-51.85%	110	47	2.34	34.69%	01/06/21	⋮
3,100.00	+1.22%	54.60	55.43	56.25	54.70	-74.75	-57.74%	775	891	0.87	34.40%	01/06/21	⋮
3,105.00	+1.06%	51.15	51.93	52.70	51.97	-70.93	-57.71%	172	47	3.66	35.14%	01/06/21	⋮
3,110.00	+0.90%	47.80	48.55	49.30	47.75	-70.65	-59.67%	234	98	2.39	33.98%	01/06/21	⋮
3,115.00	+0.74%	44.55	45.28	46.00	44.83	-63.27	-58.53%	124	46	2.70	34.22%	01/06/21	⋮
3,120.00	+0.59%	41.50	42.20	42.90	41.70	-56.30	-57.45%	380	74	5.14	34.08%	01/06/21	⋮
3,125.00	+0.43%	38.50	39.18	39.85	39.30	-65.35	-62.45%	235	100	2.35	34.60%	01/06/21	⋮
3,130.00	+0.27%	35.70	36.35	37.00	36.00	-59.60	-62.34%	465	97	4.79	34.01%	01/06/21	⋮
3,135.00	+0.11%	33.00	33.63	34.25	33.50	-61.35	-64.68%	402	38	10.58	34.15%	01/06/21	⋮
3,140.00	-0.05%	30.45	31.03	31.60	30.50	-61.80	-66.96%	804	165	4.87	33.61%	01/06/21	⋮

FIGURE 26 – Prices of some call options on the underlying asset AMZN on the platform [28]

```
##application :
"""
"""
We will calculate the price of a call option and its implied volatility.
We have chosen an option on the company Amazon.
```

```
The data on the website was used: https://www.barchart.com/stocks/quotes/AMZN/options
St =3138.38
T= 2/252 Warning, it is not the exact time, hence the error
sigma_impl =36.38%
K=3090
C=64.15
r=0.01
"""
#We calculate again the price :
prix = euro_vanilla_call(3138.38, 3090, 0.007, 0.01, 0.3460)
```

The obtained price is

$$C = 65.36\ \$$$

```
#We calculate again the implied volatility with the parameters given by the source ;
vol_impl = precision(0.0001,62.73,3138,0.007,3090,0.01)
```

We find

$$\hat{\sigma} = 0.32$$

There is a slight error in relation to the implied volatility calculated on the platform. This can have several origins : the date T is not perfectly exact here, since it is given in days, the option price (62.73)$doesnotcorrespondexactlytothatgivenbytheIt\hat{o}formula$(65.36). The results remain very satisfactory as a first approximation.

6 Conclusion

This project allowed us to study Brownian Motion in a comprehensive way. After a first physical study according to Langevin's theory and then by a mathematical characterisation, we were able to apprehend Brownian Motion in its standard and geometrical form. The experiment carried out in the laboratory allowed us to observe the Brownian Motion and to deduce an estimate of the Avogadro number. We were able to use the Brownian Motion in the modelling of the price of a financial asset. From this modelling, we derive the Black-Scholes model which allows the valuation and hedging of options. This model allows the calculation of historical and implied volatility of asset prices. The next step in the project would be to use these calculated parameters to predict the evolution of assets or derivative assets via the implementation of technical indicators for example.

7 Instructions for use

The codes corresponding to this project were realized in Python and R Studio. Thus, deliverables are available to the reader on request :

- The file `coord-tracker.xlsx` contains the X and Y coordinates of the 25 particles pointed using the Particle tracker software. The file is associated with the code `analyse_experience.R` in which we detail the calculation of the Avogadro number, the verification of the Brownian Motion hypothesis, and the simulations carried out. We can also, on request, provide the video of the microscope that allowed us to obtain the file `coord-tracker.xlsx`. These documents are placed in the `Experience_history` folder.
- The code `Prediction.R` (Appendix 8.4) which enabled the simulation given in Figure 3.7 to be carried out is located in the `Simulation` folder.
- The code `Volatilite_hist.R` (Appendix 8.3), which uses the price of a given asset to display the evolution of the temporal volatility on a grid of your choice. The code can be tested with the help of the price `AMZN.csv` also provided. As an indication, we also provide the prices of other assets in the `Finance` file.
- The code `Volatilite_impl.py` (file `Finance`) giving a strategy to calculate the implicit volatility of an underlying. The application case chosen is a call option on AMZN.

8 Appendices

8.1 Appendix 1 : Establishing the expression for Avogadro's number

If we denote

$$u(t) = \frac{1}{2}\frac{d}{dt}\left\langle \|\vec{r}(t)\|^2 \right\rangle$$

The equation 1 can be written as

$$m\frac{du(t)}{dt} = -\gamma u(t) + m\left\langle \|\vec{v}(t)\|^2 \right\rangle$$

Again using the equi-repartition theorem of energy, we find :

$$m\frac{du(t)}{dt} + \gamma u(t) = dk_B T$$

where $k_B = \frac{R}{N_A}$ and d is the number of dimensions. Solving this first-order DE with constant coefficients, we find :

$$u(t) = \frac{dRT}{\gamma \mathcal{N}_A} + \lambda \mathrm{e}^{-t/\tau}$$

where

$$\tau = \frac{m}{\gamma} = \frac{m}{6\pi\mu a} \simeq 10^{-8}s \tag{12}$$

is the relaxation time.

In a regime where $t >> \tau$ we find the expressions 4 and 5 given.

8.2 Annex 2 : Itô calculus and heat equation

Indeed, the previous equation tells us that for any bounded f function we have :

$$\mathbb{E}\left(f\left(B_T\right) \mid B_t = x\right) = \int_{\mathbb{R}} f(y)q(T-t,x,y)dy$$

It is interesting to note the predictive power of such an integral.

If we denote $p(t,x;f)$ the function

$$\begin{aligned} p(t,x;f) &= \int_{-\infty}^{\infty} f(y)q(t,x,y)dy = E\left(f\left(B_t + x\right)\right) \\ &= E\left(f\left(B_{t+s}\right) \mid B_s = x\right) = \int_{-\infty}^{\infty} f(x+y)g(t,y)dy \end{aligned}$$

this function checks (use the backward equation and the theorem of derivation under the integral sign)

$$\begin{cases} p(0,x;f) = f(x) \\ -\dfrac{\partial p}{\partial t} + \dfrac{1}{2}\dfrac{\partial^2 p}{\partial x^2} = 0 \end{cases} \tag{13}$$

To calculate $E\left(f\left(B_T\right)\right)$, it is enough to solve the partial differential equation 13 and to notice that $E\left(f\left(B_T\right)\right) = p(T,0;f)$. We can write, using $\mathbb{E}\left(f\left(B_t + x\right)\right) = p(t,x;f)$

$$E\left(f\left(B_T + x\right)\right) - f(x) = p(T,x;f) - p(0,x;f) = \int_0^T \frac{\partial p}{\partial t}(s,x;f)ds = \frac{1}{2}\int_0^T \frac{\partial^2 p}{\partial x^2}(s,x;f)ds$$

We can show easily, by calculations :

$$\frac{\partial^2 p}{\partial x^2}(t,x;f) = \int_{-\infty}^{\infty} f''(x+y)g(t,y)dy = u\left(t,x;f''\right) = \mathbb{E}\left(f''\left(B_t + x\right)\right)$$

Itô's calculation, famous in finance, allows us to generalise these notions and to solve the Black-Scholes equation given in 1.

8.3 Annex 3 : R Code, Calcul of historical volatility and the trend on a market

```
data<-read.csv(file='/Users/victorletzelter/Downloads/AMZN-2.csv',header=TRUE)

evolution_volatilite<-function(data,T=20,D=60){
#data : contains the data
#T : number of days on the window (cf vol function)
#D : number of dates in the graph

TS<-ts(data)
```

```
TSD<-as.data.frame(TS)

vol<-function(t,T=20){

  #t : date at which the volatility is calculated
  #T : nomber of days of the window

  plot(TSD$Date,TSD$Close,'l',main="Action AMZN price",xlab="Dates in days",ylab="Closure price (in
  Val<-TSD$Close
  #Val<-rev(Val) : On doit inverser l'ordre de la série temporelles si les données les plus récentes
  Val<-Val[(length(Val)-T-D+t):(length(Val)-D+t)]
  dln<-diff(log(Val))

  #hist(dln,prob=T,nclass=10,main="Histogramme dlnSt AMZN",col="#99CCFF",xlab="dlnSt",ylab="Fréquenc
  #curve(dnorm(x, mean=mean(dln),sd=sqrt(var(dln))),add=T)

  #Parameters estimation

  dt=1/252 #It is a convention : time is expressed in years (trading is open 252 days a year)
  variance<-var(dln)
  moy<-mean(dln)
  sigma=sqrt(variance/dt)
  mu<-(moy/dt)+(sigma^2)/2
  return(sigma)
}

T<-seq(1,D,1)
y<-rep(0,D)
for (i in 1:D){
  y[i]=vol(i)
}

plot(T,y,'l',main='Historical volatility (window : T days) - AMZN',xlab='Days',ylab='Volatility')
}

evolution_volatilite(data)x
```

8.4 Annex 4 : prediction of a Geometric Brownian by the heat equation

```
### Simulation of a geometric Brownian motion ### discretisation of time

Bo=0
t=seq(0,10000)
### Simulation of increments
B.acc = rnorm(10001)
### Simulation of a trajectory -> we have a BM B.sim
B.sim = Bo+cumsum(B.acc)

#For a geometric BM
sigma = 0.001
mu=0.0001

#BM simulated, one a make several as this one
S=exp((mu-sigma^2/2)*t+sigma*B.sim)


#expectancy, prediction
pred=exp(mu*t)

plot(S,type="l",xlab="In red the prediction, in black the trajectory",ylab="Ordinate axis")
lines(pred,col="red")
```

Références

[1] https://hal.archives-ouvertes.fr/hal-01283567/document

[2] https://monday.com/lang/fr/

[3] https://www.youtube.com/watch?v=RoBD1YP7Esw

[4] https://fr.wikipedia.org/wiki/Mouvement_brownien

[5] https://www.youtube.com/watch?v=4-Tas6Uw_OQ

[6] https://www.researchgate.net/publication/283144550_Application_of_Markov_Chains_and_Brownian_motion_models_on_insect_ecology

[7] https://www4.ac-nancy-metz.fr/physique/ancien_site/Tp-phys/Term/TP-fluid/visco-eau.htm

[8] https://fr.wikipedia.org/wiki/Paul_Langevin

[9] https://images.math.cnrs.fr/Qu-est-ce-que-la-theorie-ergodique.html

[10] http://perso.univ-lemans.fr/~apopier/enseignement/M1_Maths_EDP/slides_intro.pdf

[11] http://math.univ-lyon1.fr/~alachal/exposes/transp_MMCS_2011.pdf

[12] https://fr.wikipedia.org/wiki/Paul_Langevin

[13] http://physics.gu.se/~frtbm/joomla/media/mydocs/LennartSjogren/kap6.pdf

[14] https://www.abcbourse.com/apprendre/3_le_monep1.html

[15] http://www.fast.u-psud.fr/~rabaud/NotesCours_Agreg.pdf

[16] https://fr.wikipedia.org/wiki/Équation_de_Langevin

[17] https://en.wikipedia.org/wiki/Einstein_relation_(kinetic_theory)

[18] https://fr.wikipedia.org/wiki/Mouvement_brownien

[19] https://www.lptmc.jussieu.fr/user/sator/old/Chapitre2.pdf

[20] https://en.wikipedia.org/wiki/Fokker\T1\textendashPlanck_equation

[21] https://www.ks.uiuc.edu/Services/Class/PHYS498/LectureNotes/chp4.pdf

[22] https://fr.qwe.wiki/wiki/Euler\T1\textendashMaruyama_method

[23] http://www.silvere-bonnabel.com/pdf/Poly_processus_12.pdf

[24] https://www.lynxbroker.fr/portail-bourse/articles/cours-action-boeing/

[25] https://finance.yahoo.com

[26] https://www.quandl.com

[27] https://www.alphaquery.com/stock/AMZN/volatility-option-statistics/20-day/historical-volatility

[28] https://www.barchart.com/stocks/quotes/AMZN/options

[29] https://en.wikipedia.org/wiki/Black\T1\textendashScholes_model